APPARATUS AND DEMONSTRATION NOTES

Jeffrey S. Dunham, *Editor*
Department of Physics, Middlebury College, Middlebury, Vermont 05753

This department welcomes brief communications reporting new demonstrations, laboratory equipment, techniques, or materials of interest to teachers of physics. Notes on new applications of older apparatus, measurements supplementing data supplied by manufacturers, information which, while not new, is not generally known, procurement information, and news about apparatus under development may be suitable for publication in this section. Neither the *American Journal of Physics* nor the Editors assume responsibility for the correctness of the information presented. Submit materials to Jeffrey S. Dunham, *Editor.*

Realization of an optical profiler: Introduction to scanning probe microscopy

J.-M. Friedt[a)]
IMEC, Kapeldreef 75, 3001 Leuven, Belgium

(Received 7 January 2003; accepted 19 December 2003)

Scanning probe microscopy is a widely used instrumentation method based on scanning a probe over a sample to map the spatial variation of a physical property over its surface. Here we present the steps required for the realization of a generic scanning probe microscope. The selected sensor is a CD reader optical head that monitors the distance to the focusing point of a lens by which an infrared laser is focused on the reflecting surface of the sample. We thus develop an optical profiler and illustrate practical examples by mapping the topography of a coin. The focus of this article is to describe a low cost profiler illustrating all the steps of the development, from the definition of the probe of the physical property to be monitored to the result on an actual sample. © *2004 American Association of Physics Teachers.*
[DOI: 10.1119/1.1648329]

I. INTRODUCTION

Scanning probe microscopies (SPM) are used in an ever wider range of applications, from material science to biology, probing surfaces at the micrometer, nanometers, and atomic scale depending on the probe. Here we propose to tackle this subject from an experimental point of view by realizing an optical profiler that works by following a principle similar to a SPM and that requires solving the same problems as the ones encountered during the development of a SPM.

As opposed to more familiar imaging sensors such as the eye or a camera in which a large number of identical sensors work in parallel (in this example, light intensity sensors), a scanning probe microscope[1] scans a probe over a large number of distinct points in space and thus maps the spatial distribution of the physical property being analyzed. This property can be the probe–sample distance (e.g., using the tunneling current[2–6] or the force applied to a tip[7]), the local magnetic field,[8] the electrochemical current,[9] the thermal conductivity, etc.

A functional scanning probe microscope requires the solution of the following three problems:

(1) obtaining a probe–surface distance sensor with a bijectivity range as wide as possible and a noise level as low as possible in order to achieve a good vertical resolution—throughout this document bijectivity will mean that we can find a range in the probe–sample distance for which a unique measurement is obtained for a given distance, and this measurement is a unique representative of that distance;
(2) obtaining a precise positioning of the sample relative to the probe in the scanning plane;
(3) software able to move the sample relative to the probe, and for each new position read the probe–surface distance.

We will describe these steps in the realization of a profiler whose basic working principle is similar to that of the atomic force microscope (AFM). The main analysis focuses on the use of the optical head of a laser compact-disc (CD) reader[10,11] as a probe–surface distance sensor (where the probe is the lens focusing the laser). The positioning of the sample is achieved by fixing it on a digitally controlled plotter, while the software controls the various parts of the instrument.

The chronology of the development is thus the following:

(1) confirm the working condition of the optical head taken from a broken CD reader; identify the laser diode pinout and understand how to power it (Sec. II);
(2) power the laser diode properly for a stable, long term use (Sec. II A) by using the feedback of the emitted light power on the power supply voltage;
(3) detect the signal related to the distance between the focal point of the laser and the reflecting surface of the sample (Sec. II B);

(4) power the electromagnet to which the laser focusing lens is attached in order to be able to vary the probe–surface distance;
(5) accurately position the sample under the probe in order to be able to image the topography of the surface (Sec. III).

II. THE CD READER OPTICAL HEAD

The use of a CD reader optical head is an interesting, compact, and low cost option for the development of sensors requiring a light source and photodetectors (see, for example, the development of a DNA-chip[12] based on such a component).

The CD reader optical head includes a laser diode emitting in the near infrared, around 780 nm; a lens attached to a coil used as an electromagnet for varying the vertical position of the lens by varying the current flowing in the coil, as shown in Fig. 1; a four-quadrant photodetector whose signal, after proper signal processing, provides a bijective relationship with the lens–surface distance.

Following the data provided by the optical head manufacturers, the laser spot reflected from the surface after focusing by the mobile convergent lens is characterized by a diameter in the micrometer range, in our case 1.7 μm.

Since we are going to use the various parts of the optical head to construct the profiler, a good understanding of the way each part works—the power supply of the laser diode, the photodiodes, and the electromagnet coil—is required.

A. Laser power supply

The laser diode includes an emitting part and an integrated photodetector which provides an electrical signal that is a function of the emitted power (Fig. 2). Considering that the impedance of the emitting diode decreases with temperature and that the emitted power increases with the current flowing through its junctions, a constant voltage power supply would quickly lead to the destruction of the diode.

We must therefore develop an output-power controlled power supply, as shown in Fig. 3. We have achieved this result by using an operational amplifier whose stabilizing feedback loop between the output and the inverting input compares the voltage output of the integrated photodetector (which is a function of the emitted power) with a setpoint voltage. If the emitted light power is too great, the voltage obtained from the photodetector is greater than the setpoint voltage and the difference between the voltages at the inverting input V_- and the noninverting input V_+ of the operational amplifier becomes negative, $\varepsilon = V_+ - V_- < 0$, and the output voltage of the operational amplifier decreases. The opposite argument shows that if the emitted power is insufficient, the supply voltage and thus the output current of the operational amplifier increase.

The diode begins emitting laser light when the supply current reaches a value around 60 mA, as shown in Figs. 2 and 3(a). Such a current cannot be provided directly by an operational amplifier; a transistor wired in a current-amplifier configuration must be added to the output of the operational amplifier. We have chosen to use a 2N3055 power transistor, greatly oversized, in order to avoid problems related to heating that have been observed with smaller transistors. The laser power supply circuit must indeed be able to provide a stable output over several hours. Including the transistor in the feedback loop of the operational amplifier does not change the principle of the laser diode power supply circuit.

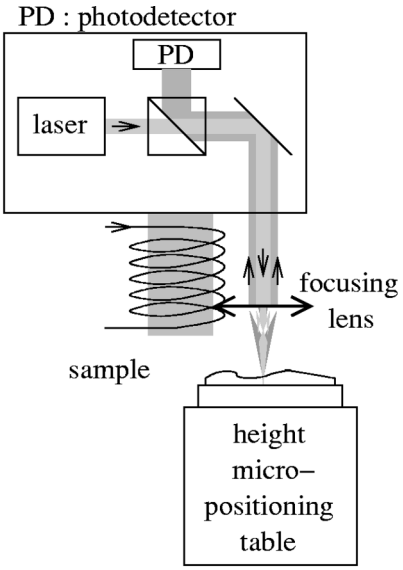

(a)

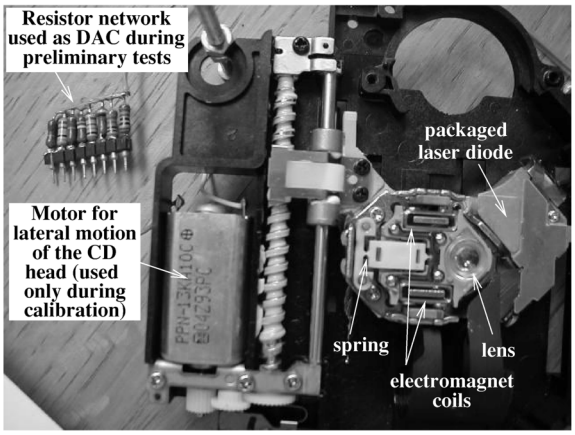

(b)

Fig. 1. (a) Diagram of the CD reader optical head: the distance between the lens and the sample can be adjusted by varying the current flowing in the coil of the electromagnet to which the focusing lens is fixed. A four-quadrant photodetector sends back an electrical signal which is a function of the distance between the focal point of the lens and the reflecting surface of the sample. (b) Photograph of one of the CD heads used during the development of this project. The motor used for positioning the head over the disc is used for the calibration as shown in Fig. 5, while the head is kept at a fixed position and the sample is scanned in mapping experiments.

The setpoint voltage required for reaching a reasonable emitted light power is obtained by *briefly* supplying the diode with an ideal voltage source through a resistor of a few hundred ohms. The light intensity emitted by the diode is first monitored using an external photodiode located under the lens of the CD reader head. A CCD sensor from a webcam can also be used for this operation if the eventual blue filter has first been removed: this filter is sometimes used to avoid saturation of the sensor by infrared sources during normal uses. Once the laser emission has been observed by the external photodiode, the voltage coming from the integrated photodetector is monitored while increasing the laser diode supply voltage: write down the value read from the photode-

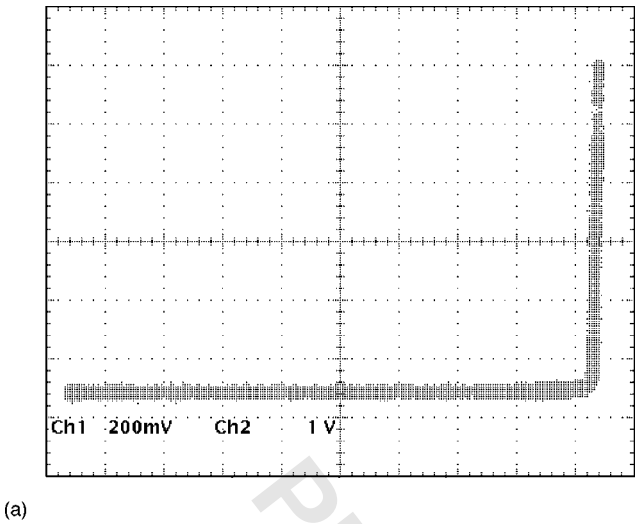

(a)

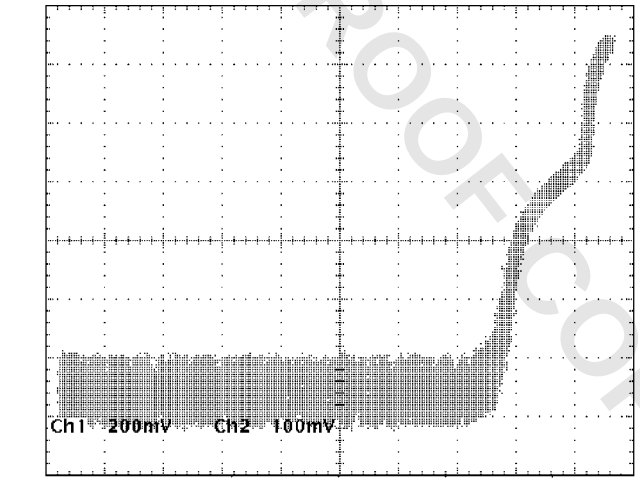

(b)

Fig. 2. (a) Intensity observed by an external photodiode located under the focusing lens, as a function of the supply voltage, and (b) photodetector response as a function of the supply voltage. In both cases the abscissa depicts the supply voltage applied through a 100-Ω resistor to pin 1 of the laser diode as shown in Fig. 3 at a scale of 200 mV/division. The ordinates display (a) the voltage at the output of a Hamamatsu S3399 silicon diode at a vertical scale of 1 V/division and (b) the output of the photodetector integrated to the laser diode for monitoring the emitted intensity at a scale of 100 mV/division.

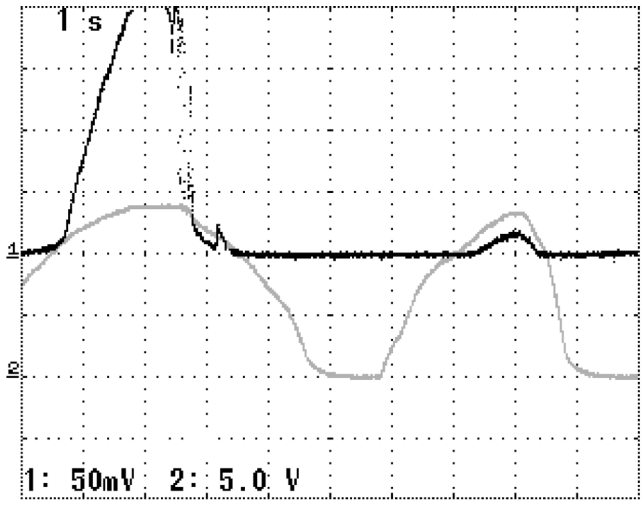

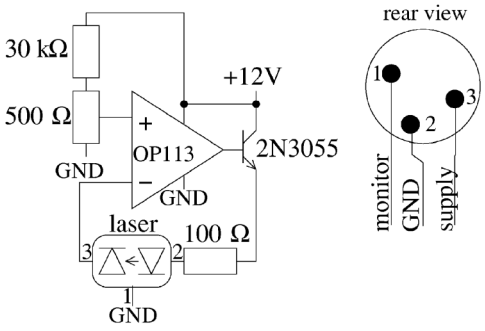

Fig. 3. (a) Laser power emitted as a function of the supply voltage applied through a 100-Ω resistor: the gray (bottom) trace is the supply voltage as a function of time depicted with an abscissa scale of 1 s/division and a vertical scale of 5 V/division. The black (top) trace is the emitted power as observed by a silicon diode Hamamatsu S3399 located under the focusing lens. Notice the fast rise of the emitted intensity when the threshold current value of around 60 mA is reached. (b) Electronic power supply circuit designed for keeping constant the emitted light intensity. The purpose of this circuit is to tune the voltage output of an OP113 op-amp (which actually is a quarter of an OP413 quad-op-amp) so that the signal read from the laser diode internal photodetector is equal to the setpoint voltage provided on the noninverting pin. The voltage at the emitter of the power transistor is measured to be around 6 V when the feedback is working properly. (c) Pinout of the laser diode, using the same pin numbering as in (b).

tector when the laser emission is clearly visible on the external photodiode. This will be the setpoint voltage to be used in the circuit described previously.

The pinout of all laser diodes tested during the development of this experiment were the same as show in Fig. 3(c). Be aware that any error in the initial connection of the laser diode will most certainly lead to its immediate destruction.

B. Using the reception photodiode quadrant

Let us remind ourselves of the working principle of a CD head in disc-reading mode. When used for reading a disc, the photodiode quadrant integrated in the CD reader head works in the following way. A four-quadrant receiving area monitors the focusing of the laser spot on the reflecting surface, and two photodetectors located on both sides of the four-quadrants sensor are used to keep the head located over the track being read.

All photodiodes are polarized by a $+5$ V voltage in order to improve their response speed to a frequency of a few megahertz. Remember that 74 min of music must fit on a 650-Mbyte disc, leading to a required bandwidth of at least 1.2 Mbytes/s$\sim$1.2 MHz.

The intensity of the light hitting the photodetectors modulates the conductivity of the photodiodes and hence varies the voltage output of the polarized photodiodes. The circuit presented in Fig. 4(a) converts the voltages W_j from the photodiodes to currents through the resistors Q_j. These currents are summed at the noninverting input V_+ and the resistor Q acts as a current to voltage converter. Finally, the op-amp converts the high-impedance input voltage V_+ to a low impedance output voltage S through the follower circuit

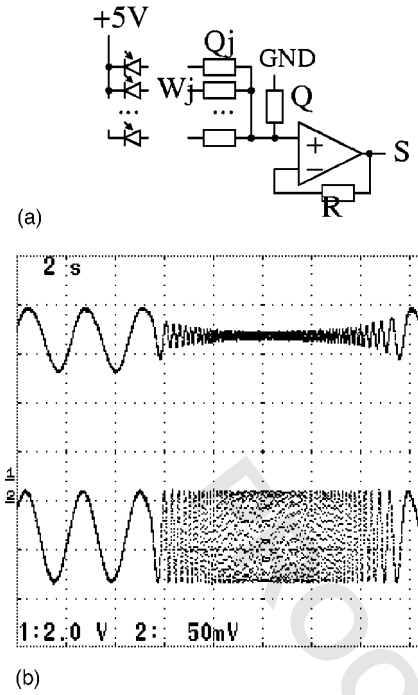

Fig. 4. (a) Circuit used to combine the signals coming from the multi-quadrants photodetector (depicted as "PD" in Fig. 1 and symbolized here by the photodiodes defining the voltages W_j) after reflection of the laser on the surface of the sample. The summation of the voltages is achieved by the resistors Q_j acting as voltage to current converters and adders, and the result is converted back to a voltage by the resistor Q. The gain of the adder is set by the feedback resistor R. This output voltage is read by an analog-to-digital converter for further processing. (b) Evolution of the signal obtained after summing the currents from the four photodiodes in the CD reader head (bottom: abscissa scale is 2 s/division, vertical scale is 50 mV/division) as a function of the frequency of the voltage driving the electromagnet (top: abscissa scale is 2 s/division, vertical scale is 2 V/division) controlling the position of the lens relative to the sample. Such a curve provides an estimate of the bandwidth of about 10 Hz and hence of the response time of the CD reader head when used in a closed loop configuration.

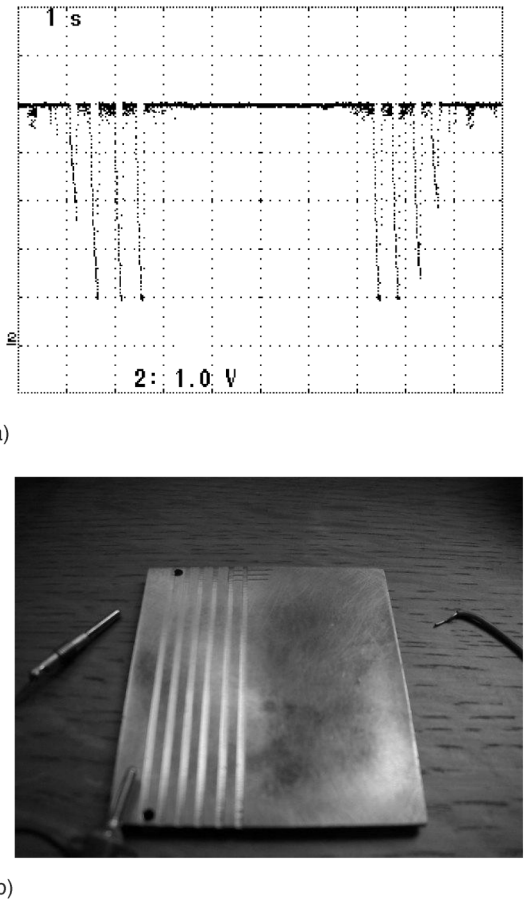

Fig. 5. (a) Display of the sum of the signals read from the four-quadrant photodiode of the CD reader head when a brass sample in which grooves of increasing depth, first with unknown depth and then from 100 to 500 μm with 100 μm steps, have been milled is scanned. This measurement provides an idea on the working range of the sensor: the signal saturates when the groove depth is greater than 300 μm, while the 100- to 300-μm-deep grooves are well resolved. (b) Photograph of the milled brass sample used for calibration: the width of the grooves is 2 mm. The scan was made from left to right and right to left, in a direction normal to the axis of the grooves.

using the resistor R (which might eventually be equal to 0). A formal analysis of the circuit using Millman theorem shows that the voltage output S is given as a function of the voltage inputs W_j as defined by the photodetectors by

$$\frac{S}{R}=\frac{\dfrac{1}{R}}{\dfrac{1}{Q}+\Sigma_{j=1}^{J}\dfrac{1}{Q_j}}\left(\sum_{j=1}^{J}\frac{W_j}{Q_j}\right). \tag{1}$$

By assuming that all resistors are chosen with the same value, i.e., that $R=Q=Q_j$, this expression is simplified to

$$S=\frac{1}{J+1}\sum_{j=1}^{J}W_j. \tag{2}$$

We check that this circuit indeed sums the intensities read from the diodes. However, as opposed to the purpose for which the photodetector quadrant was designed in which the astigmatism of the focusing lens is used to generate patterns on the photodetectors characteristic of the distance of the focus point to the surface of the sample, we here simply sum the signals obtained from the diodes. One should theoretically add the signals from diagonally opposed diodes, and subtract the resulting two signals, but it was observed experimentally that a sum of all the signals provided better results.

Although we have illustrated Eq. (1) by taking $Q_j=Q$ to make it easier to interpret, we have actually chosen $Q\gg Q_j$ so that the sum of the currents is converted to a voltage high enough to be usable: we have used $Q=1\,\mathrm{M}\Omega$ and $Q_j=560\ \Omega$ in our circuit.

A signal that is a function of the lens–sample distance is thus generated as shown in Fig. 4(b).

C. Estimate of the working range of the sensor

A first quick analysis using the dc motor that controls the lateral position of the CD reader head shows that the open-loop measurement range as obtained by only reading the signal output from the photodiodes without feedback control of the lens–sample distance is quite restricted, of a few hundreds of microns at most. The graph presented in Fig. 5 demonstrates that the laser diode-photodetector quadrant set is working properly.

III. THE PLOTTER

Once the vertical distance sensor has been installed and calibrated, a second issue related to the lateral displacement of the sample relative to the probe arises. This part can be made independent of the previous one by keeping the probe fixed and by translating the sample. This option is the one used in many implementations of the AFM since it decouples the horizontal positioning of the sample and vertical positioning of the probe.

We have in this setup used a second-handed plotter, a Roland DXY-1200, which provides a lateral resolution of 25 μm and can be digitally controlled with an RS232 serial link at 9600 baud. The language used to control the plotter, HPGL, is well documented and easy to use.[13] This solution is easier to implement than using an analog plotter[1] which requires two additional digital-to-analog converters and does not guarantee a constant lateral resolution.

The only HPGL commands useful in this application are `PU`; for raising the pen-holder (and hence bring the sample to a pre-defined height), `PAx,y` to bring the sample to the position (x,y) preliminarily defined where the CD reader head was positioned, and finally `PRx,y`; to move the sample a distance (x,y) relative to its current position. This latter command is used with the sets $(\pm 1,0)$ during a line scan with a 25 μm/pixel resolution and (0, 1) to switch to the next line. All the x and y values are in units of 25 μm/pixel.

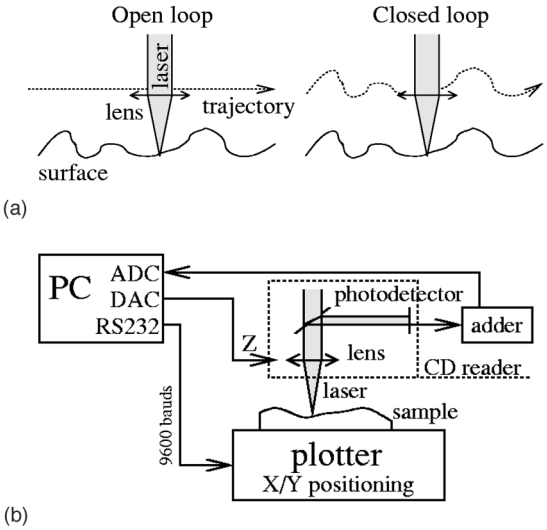

Fig. 6. Two modes for operating a scanning probe microscope: (a) in the open loop configuration, only the value coming from the detector being recorded, and (b) the closed loop configuration, the value read from the sensor being kept constant to a setpoint value by varying the probe–surface distance). (c) Experimental setup: an IBM compatible personal computer fitted with an analog-to-digital converter (ADC) and digital-to-analog converter (DAC) monitors the output of the CD-head photodiodes and controls the lateral position of the sample under the focusing lens in a raster scan motion.

IV. THE SOFTWARE

We identify two modes for using an AFM which we call open loop and closed loop operations. In the former, the probe is positioned at the beginning of the scan at a given distance from the surface of the sample where the signal–distance function displays a maximum slope in a bijectivity range, and then the sample is moved and the signal coming from the probe is recorded for each new position. In the latter, the vertical position of the probe is adjusted for each new point of the sample to be analyzed in order to get a signal from the probe equal to a setpoint value, and the height command sent to the probe is the recorded signal. This second operation mode, although more difficult to implement and thus slower, provides two advantages. First, the linearity of the recorded signal is no longer dependent on the physical property being measured (which the experimenter usually cannot control) but on the actuator controlling the height of the probe. Second, the vertical range in which the profiler can be used is greatly increased since it is no longer limited by the bijectivity region of the signal–distance relationship, which is itself dependent upon the physical property being monitored. Instead of requiring that the probe–sample distance stays within the bijectivity range over the *whole* area under investigation, this condition only has to be verified for every two *successive* points.

In this example, we observe that by moving a front-coated mirror in front of the laser focusing lens that the signal read by the photodetector only varies with distance over a range of a fraction of a millimeter, which requires a very precise adjustment of the parallelism between the average plane of the surface to be scanned and the plane in which the sample is translated. In a closed loop configuration, the actuation range of the lens and the application range of the profiler is greatly increased to a few millimeters thanks to the electromagnet.

Going from a sensor indicating with good accuracy the distance from the surface of the sample to a functional scanning-probe microscope requires some digital electronics and software development, as shown in Fig. 6(c). The signal coming from the multi-quadrant photodetector is converted to a digital signal using a 12-bit resolution AD574 analog-to-digital converter (ADC) installed on an ISA card. The command controlling the position of the electromagnet is sent to a 16-bit resolution AD669 digital-to-analog converter (DAC) on an ISA card. The software, written in TURBO PASCAL under DOS, is used to read and store the topography data as well as to synchronize the data acquisition with the translation of the sample as described in Fig. 7.

An alternative to the development of data acquisition and control cards to be connected to the ISA bus of a PC is the use of a microcontroller. A wide range of such chips is now available which only require a limited number of peripheral components to run, ofter providing analog-to-digital conversion while the digital-to-analog can be built cost-effectively with a network of resistors. The Motorola 68HC11F1 or Hitachi H8/3048F microcontrollers do not require any specific programmer as they can be programed directly from a standard RS232 port from a PC and are equipped with the required converters for this experiment as well as with a serial port to send commands to the plotter. The development of test circuits for these microcontrollers is beyond the scope of this note: the reader interested in such topics is referred to the documents available at Ref. 14 for further information.

A. Open loop measurements

In order to be able to make open loop measurements, the surface to be scanned must first be positioned under the lens of the CD reader head. Its height is then adjusted while the analog-to-digital converter displays the values read on the output of the photodetector; when a variation of the values becomes visible while the lens–surface distance varies, a us-

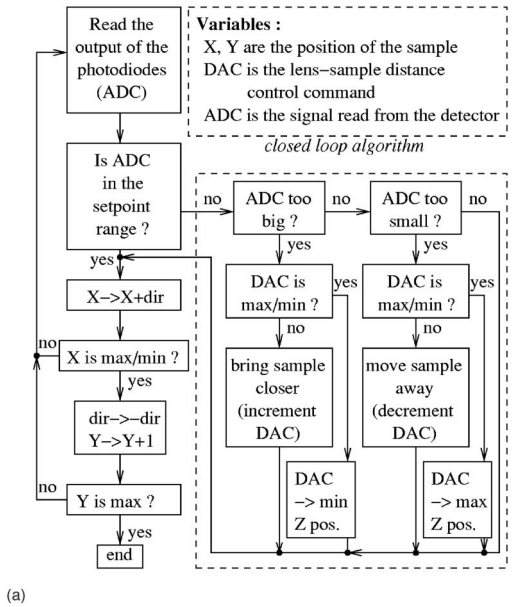

(a)

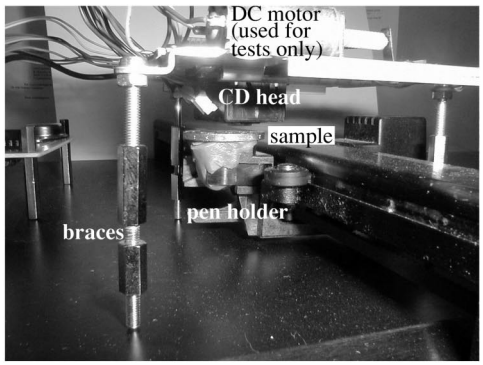

(b)

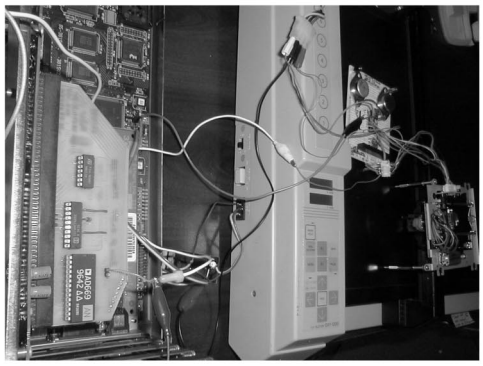

(c)

Fig. 7. (a) Algorithm for controlling the instrument. ADC depicts the reading of the analog-to-digital converter, proportional to the sum of the currents going through the photodiodes. When using the open loop operation mode, the value coming from the sensor is recorded, while in the closed loop operation mode we record the current running through the coil of the electromagnet as controlled by the DAC with the ADC being equal to the setpoint value. Photographs of the experimental setup: (b) a closeup side-view of the plotter pen-holder to which the coin is fixed using modeling clay as seen on the center of the picture, while the sensor is held over the sample by braces resting on the surface of the plotter for easy adjustment of the height of the CD head and its parallelism with the average plane of the sample. (c) The personal computer controlling the experiment is visible on the left of this top-view photograph, including the AD669-based digital-to-analog conversion ISA card, while the plotter and the electronic circuits related to the laser diode, including the two large 2N3055 power transistors, are visible to the right. The sensor resting over the sample is visible on the far right of this photograph.

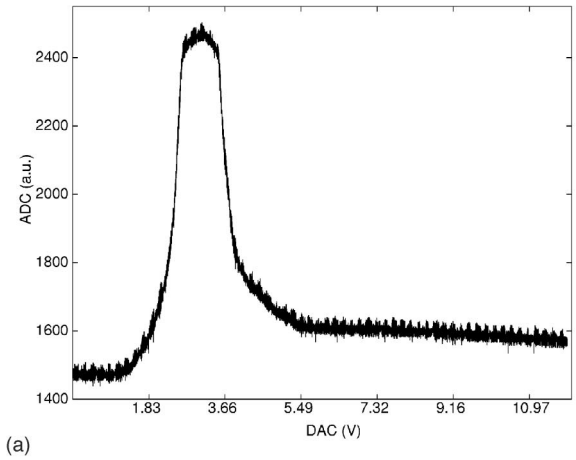

(a)

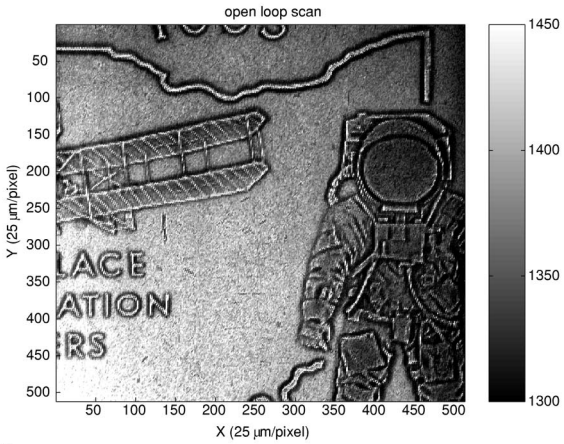

(b)

Fig. 8. (a) Signal–distance relationship and (b) topography of a 25 cent American coin obtained using the open loop algorithm. The peak in the signal–distance curve (a) indicates the position of the coil, as controlled by the DAC, for which the laser is focused on the surface and therefore for which the signal detected by the photodiodes is greatest. The region where the slope of this peak is greatest, for a DAC voltage ranging from 3.5 to 5.5 V here, will lead to the sharpest contrast in the topography image during the scan.

able working setpoint has been reached. Best results are obtained when the setpoint is located on the steepest slope of the signal–distance relationship, located in the middle of the bijective region of this function. The position of the lens is then set, as well as the height of the sample, and the analysis of the sample simply involves translating the surface laterally and monitoring the output of the photodetector for each new position.

Once the scan is completed, we obtain a file including an $N \times N$ matrix which is displayed as a topographic image using the MATLAB function `imagesc` as displayed in Fig. 8.

This imaging mode illustrated in Fig. 6(a) is fast but limited by the sensitivity range of the sensor: if the surface to be analyzed is rougher than this sensitivity range, i.e., the surface comes too close or too far from the lens, the resulting image is saturated, and data on the surface are missing. This problem is worse in the case of an AFM since a surface getting too close to the tip might damage the probe or destroy it by applying too high a force. Furthermore, the force applied to the tip by the sample is not controlled and thus is not constant, leading to nonlinearities in the force–distance relationship, e.g., the forces become attractive or repulsive

depending on the distance. As can be seen in Fig. 8(a), the signal–distance relationship is not linear and a calibration relating the measured signal to a physical height is not possible.

B. Closed loop measurements

In this mode, illustrated in Fig. 6(b), instead of keeping the height of the lens constant, the coil electromagnet affixed to the lens is connected to a digital-to-analog converter in order to be able to track the profile of the surface by keeping the signal from the photodiodes constant. Since the output impedance of the DAC or of an operational amplifier used in a follower configuration is too high, a 2N3055 power transistor mounted in current amplifier configuration is added to drive the electromagnet.

This mode is slightly slower than the previous one since it requires an adjustment of the height of the coil for each new point on the surface, but the resulting image is no longer dependent on the signal–distance relationship but only on the actuator–distance relationship, which is much easier to control. Furthermore, the range over which data can be collected is only limited by the means for actuating the lens, which provides an amplitude of a few millimeters in the case of the electromagnet used in the head of a CD reader. The result of such a closed loop scan is presented in Fig. 9.

Of particular interest to us here, the open loop images are of better quality than the images obtained in the closed loop configuration. We attribute this result to the fact that the actuator (the electromagnet controlling the position of the lens) is not appropriate for our application and does not improve the dynamics of the signal, i.e., its operating range, or the linearity of the distance–signal relationship. Furthermore, the limited bandwidth of the reader head implies that a longer delay is needed than the one we used for the position of the lens to stabilize above the sample during the feedback loop. The version of the data acquisition software used here doesn't include any delay between the actuation of the electromagnet and reading the value at the output of the photodiodes, since the acquisition of a whole image is already a very slow process. We still gain in resolution when switching from the open to the closed loop algorithm since the data saved for displaying the topography improve from a 12-bit ADC resolution to a 16-bit DAC resolution. As opposed to the open loop configuration where the relationship between the recorded signal and the topography is dependent on the linearity of the transducer, we can now assume for the closed loop configuration that the displacement of the electromagnet is proportional to the DAC output and provide a proportionality factor between the recorded signal and the topography. The calibration was done using a Veeco Dektak 3030: the height difference between the background plane and the helmet of the astronaut shown in Fig. 9(b) ranges from 87 ± 15 μm (part of the helmet closest to the center of the coin) to 107 ± 10 μm (part of the helmet closest to the border of the coin), leading to a signal to height proportionality factor of 27.5 ± 0.3 DAC units/μm or 10.2 mV/μm for a 16-bit DAC with a ± 12-V output range.

We will not describe here the various image-processing steps that are often used to improve the quality of the topographic image acquired. Let us just warn the reader of the risks of generating artifacts when using advanced processing methods. All the images presented in this document are raw data and no data processing has been used for improving the images.

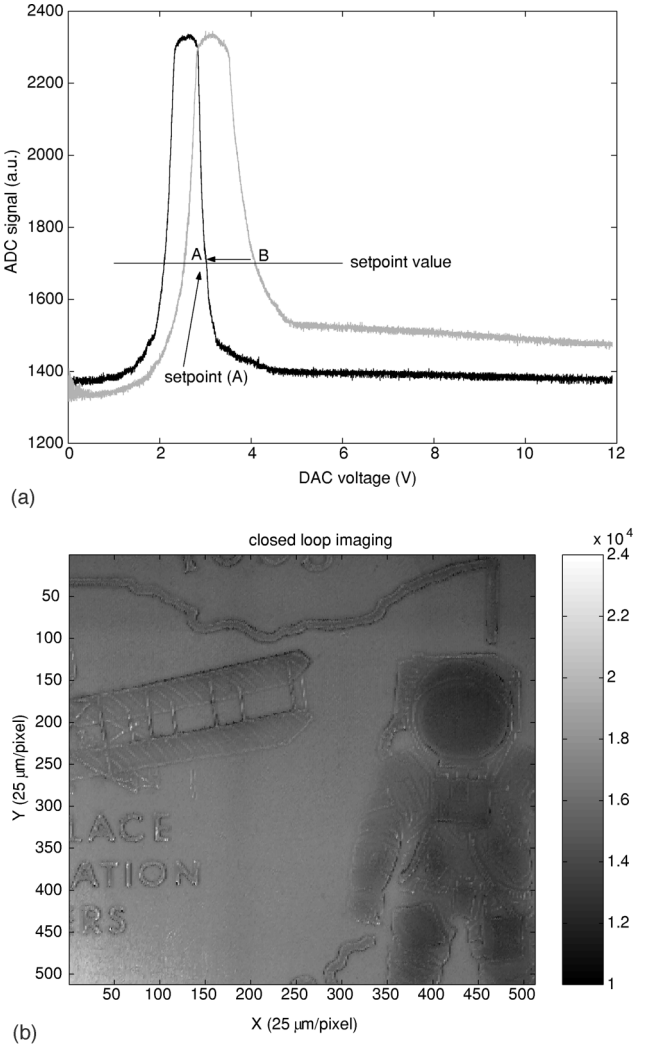

Fig. 9. (a) Signal–distance relationships for two different positions of the lens over the surface and (b) topography of a 25 cent American coin obtained using the closed loop algorithm. While in Fig. 8(a) the signal–distance relationship only provides a calibration information, we here observe how the signal–distance relationship varies over different points of the surface and how the closed loop algorithm, by varying the lens–surface distance, aims at keeping the ADC voltage fixed at the setpoint value represented by point *A*. The objective of the closed loop algorithm is to move the lens so that point *B* comes to the position of point *A* and hence that the gray signal–distance curve overlaps the black one. The control signal applied to the DAC to reach this condition is recorded and plotted on image (b) for all scan positions.

V. CONCLUSION AND PERSPECTIVES

We have used the optical head of a CD reader for building an optical profiler. We have thus been able to experiment with the actual steps to be followed during the realization of any scanning probe microscope. We have described the various steps for assembling the probe as well as the positioning of the sample relative to the probe, and finally seen what the different operating modes of this instrument are.

In the same way that the first AFM was an extension of the scanning tunneling microscope, it would be possible to im-

prove the lateral resolution of the apparatus described here by including an intermediate probe between the surface and the laser spot. In this case, the laser spot would be used to detect the deflection of a cantilever similar to the one used in an AFM, the latter being directly sensitive to the forces applied by the surface to the tip. This kind of improvement by adding an intermediate probe opens a wide range of possible extensions of the instrument by choosing an appropriate probe for detecting a physical property other than the topography of the sample.

ACKNOWLEDGMENTS

I thank C. Ferrandez (LPMO/CNRS, Besançon, France) for initial discussions on this project, and L. Francis (IMEC, Leuven, Belgium) for the calibration measurements.

[a]Electronic mail: friedtj@imec.be

[1]R.A. Young, ''Quantitative experiments in electric and fluid flow field mapping,'' Am. J. Phys. **69** (12), 1223–1230 (2001).

[2]R.J. Behm, N. Garcia, H. Rohrer, and T.G. Vold, ''Scanning Tunneling Microscopy and Related Methods,'' Am. J. Phys. **59** (8), 765 (1991).

[3]R.A. Lewis, S.A. Gower, P. Groombridge, D.T.W. Cox, and L.G. Adorni-Braccesi, ''Student scanning tunneling microscope,'' Am. J. Phys. **59** (1), 38–42 (1991).

[4]C. Julian Chen and W.F. Smith, ''Introduction to Scanning Tunneling Microscopy,'' Am. J. Phys. **62** (6), 573–574 (1994).

[5]P.J. Williams, D. White, K. Mossman, S. Walker, and G.P. Cant, ''A simple scanning tunneling microscope,'' Am. J. Phys. **65** (2), 160–161 (1997).

[6]G. Binnig, H. Rohrer, Ch. Gerber, and W. Weibel, ''Surface Studies by Scanning Tunneling Microscopy,'' Phys. Rev. Lett. **49** (1), 57–61 (1982).

[7]G. Binnig, C.F. Quate, and Ch. Gerber, ''Atomic Force Microscope,'' Phys. Rev. Lett. **56** (9), 930–933 (1986).

[8]Y. Martin and H.K. Wickramasinghe, ''Magnetic imaging by 'force microscopy' with 1000 Å resolution,'' Appl. Phys. Lett. **50** (20), 1455–1457 (1987).

[9]A.J. Bard, F.R.F. Fan, J. Kwak, and O. Lev, ''Scanning Electrochemical Microscope. Introduction and Principles,'' Anal. Chem. **61**, 132–138 (1989).

[10]J.P. McKelvey, ''Kinematics of the Compact Disc/Digital Audio System,'' Am. J. Phys. **53** (12), 1160–1165 (1985).

[11]K.C. Pohlman and T.D. Rossing, ''The Compact Disc,'' Am. J. Phys. **58** (1), 94 (1990).

[12]F. Perraut Francois, A. Lagrange, P. Pouteau, O. Peyssonneaux, P. Puget, G. McGall, L. Menou, R. Gonzalez, P. Labeye, and F. Ginot, ''A new generation of scanners for DNA chips,'' Biosens. Bioelectron. **17** (9), 803–813 (2002); `http://www-leti.cea.fr/Commun/Revue_Annuelle/biology&health/FGINOT.PDF`

[13]`http://astronomy.swin.edu.au/~pbourke/geomformats/hpgl/`: a brief presentation of the HPGL language, including the main commands and their syntax.

[14]`http://friedtj.free.fr`: includes tutorials for low cost microcontroller development projects based on the Linux operating system and OpenSource development tools.

PROOF COPY 007404AJP